Acta Astronautica 99 (2014) 143–152

Contents lists available at ScienceDirect

Acta Astronautica

journal homepage: www.elsevier.com/locate/actaastro

Experimental investigation on shock wave diffraction over sharp and curved splitters

F. Gnani *, K.H. Lo, H. Zare-Behtash, K. Kontis

University of Glasgow, School of Engineering, Glasgow G12 8QQ, UK

ARTICLE INFO

Article history:
Received 21 November 2013
Received in revised form
23 January 2014
Accepted 21 February 2014
Available online 27 February 2014

Keywords:
Shock wave
Shock–vortex interaction
Fluid dynamics

ABSTRACT

Shock wave diffraction occurs when a normal travelling wave passes through a sudden area expansion. Turbulent, compressible, and vortical are the characterising adjectives that describe the flow features, which are slowly smeared out due to the dissipative nature of turbulence. The study of this phenomenon provides insight into several flow structures such as shear layer formation, vortex development, and vortex/shock interaction whose applications include noise control, propulsion or wing aerodynamics. A large amount of research has been carried out in the analysis of shock wave diffraction mainly around sharp wedges, but only few studies have considered rounded corners. This project has the aim to examine and compare the flow features which develop around three different geometries, ramp, symmetric and rounded, with experimental incident shock Mach numbers of 1.31 and 1.59, and Reynolds numbers of 1.08×10^6 and 1.68×10^6. Schlieren photography is used to obtain qualitative information about the evolution of the flow field. The results show that ramp and symmetrical wedges with a tip angle of 172° behave in the same manner, which exhibit clear dissimilarities with a curved corner. The flow field evolves more rapidly for a higher incoming Mach number which is also responsible for the development of stronger structures.

1. Introduction

The basic physical principles of the shock wave diffraction phenomenon have been studied in a wide range of corner angles and flow speeds reporting numerous phenomena, but mainly focused on sharp geometries [1–4]. Mach numbers slightly higher than 1.0 and less than 2.0 have acquired particular importance in research since vortex effects in this condition influence the behaviour of compressible flows over solid surfaces, the performance of aerodynamic flow devices and, in general, flight vehicles. The vorticity production is small [5] and the flow features are completely developed with a well-defined vortex which, as reported by Skews [1], start to spread out for Mach numbers greater than 2.0.

A schematic of the flow features characterising Mach numbers less than 1.45 is illustrated in Fig. 1(a). The region bounded by the planar incident shock wave, its weakened part, consisting in the curved diffracted shock wave (in the upper side of the picture) and the reflected expansion shock wave (in the lower side) was called the perturbed region by Skews et al. [6] and remains subsonic for an incident Mach number less than 2.068.

For incident Mach numbers in the range 1.3–1.5 Skews et al. [6] showed that, with wedge angles greater than 20°, separation starts to appear becoming clearly visible at 30°, when the presence of transonic lambda shock structures on the shear layer can be distinguished. For greater angles the arrangement of the developed shock waves varies, but reaches a limiting configuration at a critical angle of 75°, over which the flow features become independent of the geometry [1].

The presence of the wall impacts the flow field development due to the shock/wall interaction, not only at

* Corresponding author.
E-mail address: f.gnani.1@research.gla.ac.uk (F. Gnani).

http://dx.doi.org/10.1016/j.actaastro.2014.02.018
0094-5765

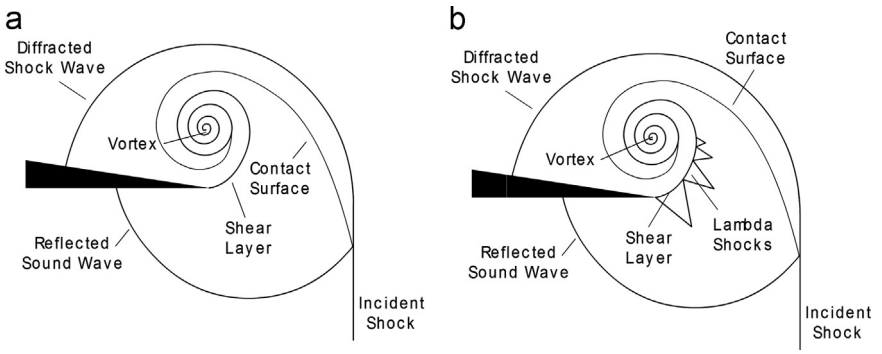

Fig. 1. Flow feature of diffraction around a sharp wedge at (a) $M = 1.31$; (b) $M = 1.59$.

moderate convex corners but also in curved geometry profiles. A zone of recompression shock between the main vortex and the wall has been observed by Quinn [7] and the experimental investigation conducted by Skews [8] led to the conclusion that the change in radius has no effect on the overall flow pattern.

Besides the geometry of the splitter, another parameter that affects the flow evolution is the incident Mach number. Skews [1] reported that, for a wide range of corner angles, in the subsonic range the region perturbed by the presence of the wall exhibits a weak density variation with a small vortex at the corner, and the process can be considered isentropic. For slightly increased Mach numbers, the flow features become stronger and a feeble appearance of the shear layer indicates the inability of the flow to negotiate the corner. The region occupied by both the slipstream and the vortex is characterised by large gradients in density, experimentally observed by Abate and Shyy [9] and was found to be more turbulent and wider for smaller corner angles [1].

Small vortices form on the shear layer generating the typical Kelvin–Helmholtz instability structure due to the growing interaction between the viscous effect and the baroclinic effect, numerically investigated by Sun and Takayama [2] but never observed experimentally before. The authors attributed this to a non-physical phenomenon, however later Quinn and Kontis [10] experimentally demonstrated that the numerical findings were actually correct.

Analytical investigations have been carried out by Skews [11] to study the point of intersection between the incident wave and the reflected sound wave, shown in Fig. 1. The shape of the diffracting shock wave has been extensively studied using Whitham's theory, [12,13,15,14] however the comparison with experimental results showed some discrepancies, forcing researchers to introduce modifications. Skews [11] found the assumption that the diffracted wave is continuous but not true. Abate and Shyy [9] stated that, during the expansion, the shock wave curvature makes a variation of the shock strength which then produces the variation of pressure and density across it. Skews [8] later confirmed that at the wall the diffracted wave is of finite strength and does not weaken to a sound wave. The point of inflexion of the diffracted shock wave was predicted by the linearised Lighthill's theory [16] for incident Mach numbers between 1.0 and 4.0 and angles at the corner in the range 15–165°. For greater Mach numbers the point of inflexion tends to transform into a triple point detached from the wall for angles in the range 60–90°. However with corner angles between 120° and 170° no triple point occurs, as observed in the work of Bazhenova et al. [15]. Srivastava [17] recently performed an analysis extending the theory which relates the curvature of a normal diffracted shock with the vorticity distribution to any corner angle since previous theories were applicable only for small or large corner angles separately.

Fig. 1(b) illustrates the case for Mach numbers greater than 1.45 where the incoming flow expands, becoming locally supersonic in the vicinity of the corner, leading to the development of the typical lambda shock structure on the shear layer. This phenomenon, which was detected by Skews et al. [6] for an incident shock Mach number $M \geq 1.35$, becomes stronger and more visible as the shock strength increases [18].

Mach numbers in the range 1.6–1.87 introduce a new flow peculiarity, called terminator, which consists of a discontinuity developed at the corner and supposed to be the tail of the Prandtl–Meyer fan [1]. In this Mach numbers range also secondary and tertiary shocks form after the lambda shocklets on the slipstream, decelerating the supersonic flow around the vortex. The threshold of the formation of the secondary shock was found by Sun and Takayama [3] to be dependent on both the corner angle and the incident Mach number.

Mach number of 2.0 is the boundary of the propagation of the reflected sound wave, which starts to be swept downstream since the gas flow behind the incident shock is approximately sonic; no additional flow features appear for Mach numbers greater than 3.0. [1]

Although in the last half-century the technology advancement has given a massive contribution to the development of experimental apparatus, the complexity of the flow scenario and the small time scale have made the capture of the processes extremely difficult. This study analyses with the schlieren technique the whole flow evolution around 172° corners of ramp and symmetrical shapes along with a curved geometry with a 2.8 mm radius. The flow features of the three geometries are compared for Mach numbers of 1.31 and 1.59.

2. Experimental setup

2.1. Shock tube and test section models

The shock tube, identical to that employed by Gongora Orozco et al. [19,20], consists of a shock tube of square cross

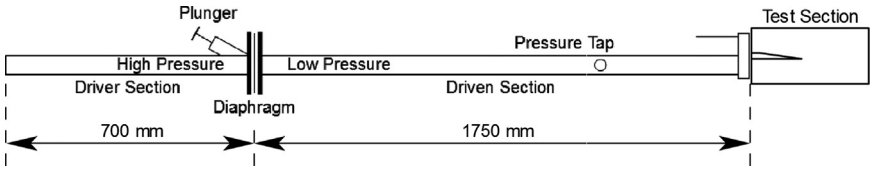

Fig. 2. Schematic of the shock tube.

sectional area with an internal section of 24.8 mm and wall thickness of 2.6 mm. The driver and driven sections were 700 mm and 1750 mm long respectively. The pressure in the driver section was monitored using a Kulite XTL-190 transducer whereas the gas in the driven section was at ambient conditions. As the schematic of the shock tube illustrates in Fig. 2, the two sections are initially separated by an acetate film ruptured with a spring-loaded plunger pointing to the middle of it. The thickness of the diaphragm was 19 and 75 μm to sustain the pressure ratio that generates an incident shock Mach number of 1.31 and 1.59 respectively. The Reynolds numbers based on the diameter of the duct are 1.08×10^6 and 1.68×10^6. A planar shock wave normal to the walls is suddenly produced and travels along the tube finally reaching the test section. The details of the three test models used and the sizes of the optical section are given in Fig. 3.

2.2. Schlieren

The arrangement of the schlieren system is the Z-type configuration identical to that used by Zare-Behtash et al. [21,22] A continuous light beam, obtained from a 450 W Xenon arc lamp, passes through a slit and a condenser lens with a 79 mm focal length before being collimated with a parabolic mirror of 203.3 mm diameter and 1016 mm focal length. The light beam then illuminates the test section and is focused by another parabolic mirror, a knife-edge and a focusing lens of 49 mm diameter. A Photron SA1.1 high-speed camera, with a 12-bit dynamic range, is used to record data with a frame rate of 16,800 fps and an exposure time of 1 μs.

The photographs were processed with ImageJ. A reference image, corresponding to the wind-off condition (no flow), was subtracted from the wind-on images in order to remove the imperfections on the test section windows as well as non-uniformities in the illumination.

Schlieren methodology was employed by Quinn and Kontis [10] who observed that, as the vortex develops, the flow behaviour and the instabilities under the corner are quite difficult to be detected due to a large density gradient, and Skews [1] was not able to observe the lambda shocklets on the shear layer.

3. Results and discussion

3.1. Ramp geometry

The reference time $t_0 = 0$ for each set of schlieren images is taken as the image before the shock wave arrives at the corner. Fig. 4(a)–(c) qualitatively depicts the initial stages of the flow evolution for a Mach number of 1.31 and the ramp model. As soon as the incoming flow passes the corner, it diffracts forming the typical structure with the

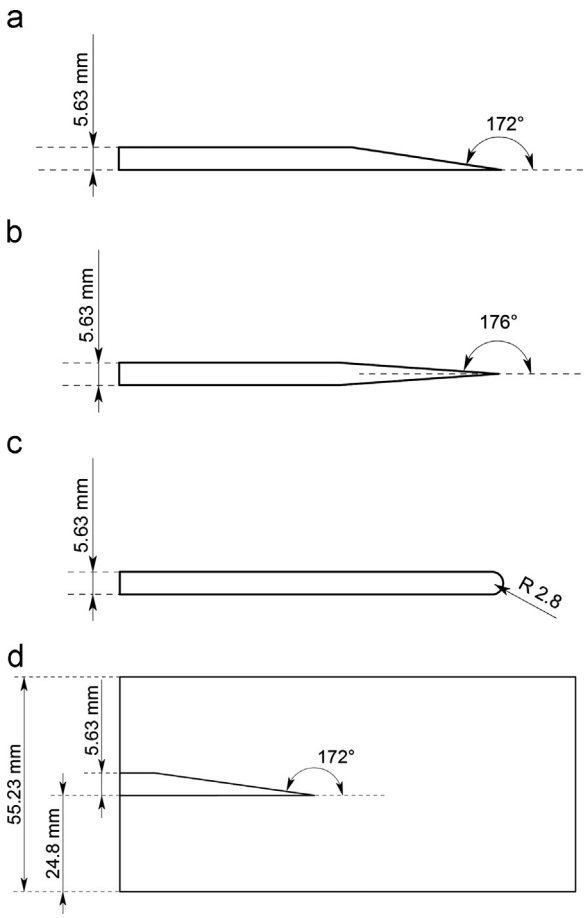

Fig. 3. Geometry of the test models. (a) Ramp; (b) symmetric wedge; (c) rounded geometry; (d) optical section.

curved diffracted shock, *DS*, and the reflected expansion wave, *ES*, starting from the opposite surfaces of the splitter and meeting the incident shock, *IS*, at the same point. The flow bounded by these two waves has been analytically found to be subsonic employing the one-dimensional equations of continuity, momentum and energy for unsteady flows [23,24]. The acoustic expansion wave propagates upstream while increasing the size for both the Mach numbers tested, in agreement with Skews et al. [6] The expansion wave meets the incident shock at the point where the curvature of the diffracted shock starts, as the normal portion of the incident wave is not affected by the presence of the corner. In the same intersection point the contact surface, *CS*, originates, which consists of the separation between the flow passing through the

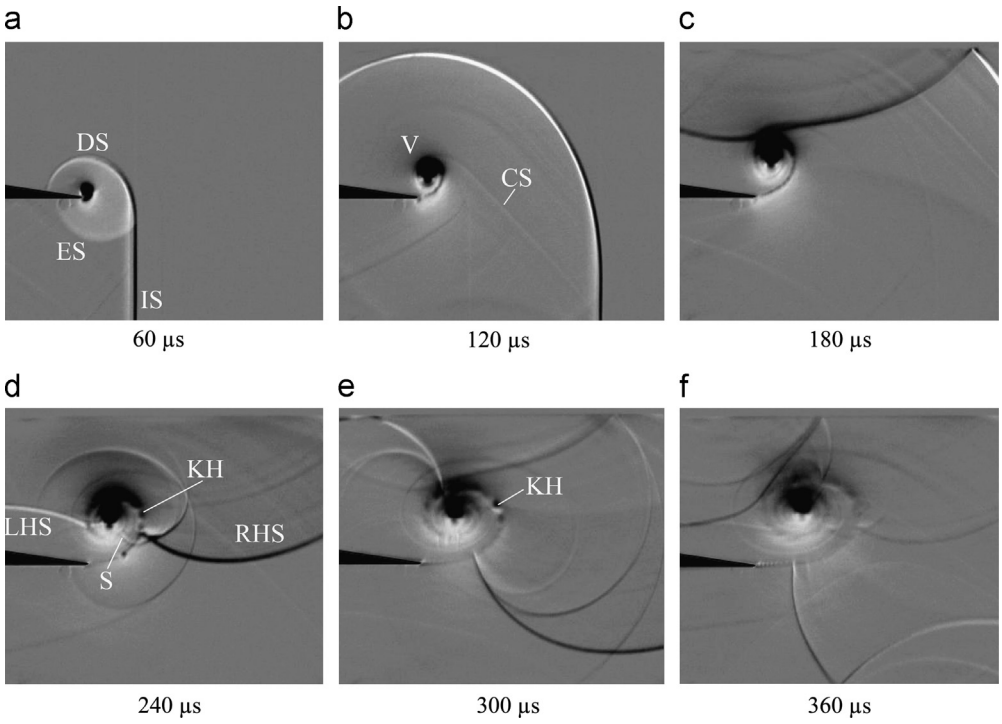

Fig. 4. Schlieren sequence of diffraction with an incident Mach number of 1.31 around a ramp corner.

normal shock wave and the flow exposed to the curved expansion shock.

The inability of the high-speed flow behind the incident wave to negotiate the corner, due to the change in density and therefore the presence of an adverse pressure gradient, provokes the flow detachment from the surface and the formation of a slipstream, which rolls up into a vortical structure, *V*, where the contact surface also terminates [1,8]. The shear layer is a narrow surface of finite thickness that separates the stationary flow in the expansion region from the high-speed incident wave, and thus makes a discontinuity in the tangential velocity [3]. The geometric effect on the formation, propagation and decay of the slipstream and the vortex were performed by Zare-Behtash et al. [21,22] with different shapes, sizes and flow Mach numbers. The nozzle lip influences the shock diffraction process and was identified to the point near which the vortex instabilities develop.

The low speed of the incident flow generates only a Prandtl–Meyer fan which continuously expands the flow on the slipstream. However, as illustrated in Fig. 5(a)–(c), a higher incident Mach number induces the flow on the shear layer to locally reach a supersonic speed and a train of small lambda shocks, *TL*, starts to form on the outer side of the slipstream perpendicular to it from the early stages of the shock wave diffraction, becoming discernible in Fig. 5(b) and (c). This structure, which is due to the acceleration of the flow that is not correctly expanded, occurs on the corner tip, progressively reducing its size and terminating at approximately 90° around the vortex in a region of high density which produce the intensity variations in the schlieren pictures. It can also be noted that the last shocklet exhibits a stronger interaction with the mainstream identified by a steeper contrast in the image.

The diffracted shock reflects from the upper bounding wall and travels back towards the vortex core, for Mach number of 1.31, which is shown in Fig. 4(d)–(f). The reflected diffracted shock, in its motion towards the vortex, is subject to a visible distortion due to the velocity field created by the vortex rotation which then leads to the generation of two split shock waves, namely an accelerated shock (on the left-hand side of the vortex) and a decelerated wave (on the right-hand side).

After having reflected from the upper surface of the splitter, in Fig. 4(d), the left-hand wave, *LHS*, opposes the vortex rotation and symmetrically travels around the vortex respect to the shock on the right-hand side, *RHS*. This leads to a pressure distribution that generates diverging acoustic waves starting on the shear layer, similar to what is described by Chang and Chang [25] and a schematic is given in Fig. 6(a). The flow on the right-hand side initially forms a Mach reflection on the slipstream in the presence of an additional stem, *S*, which penetrates the shear layer and terminates in the internal part of it. This stem however appears to be independent of the rest of the structure, travelling faster and generating weaker waves as the vortex develops further enlarging its shape, as illustrated in Fig. 4(e) and (f).

The interaction of the vortex with the returning diffracted shock is sufficiently weak to not affect it and appears to be the reason for the formation of small vortices, *KH*, on the shear layer which starts from the splitter tip to around 120° around the vortex in Fig. 4(d), until the schlieren image does not allow us to visualise

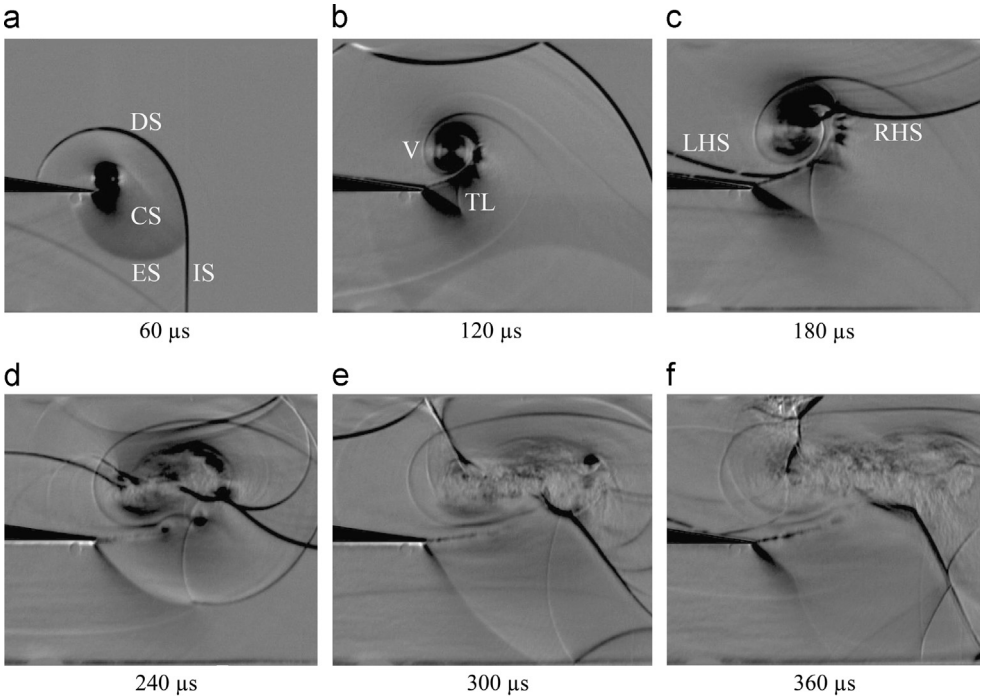

Fig. 5. Schlieren sequence of diffraction with an incident Mach number of 1.59 around a ramp corner.

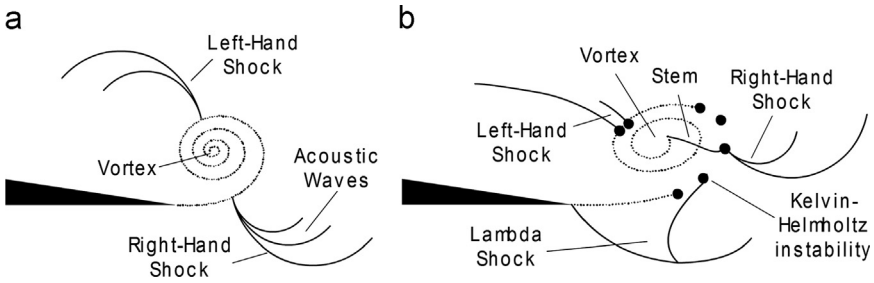

Fig. 6. Schematic of the vortex/shock interaction for a sharp wedge at (a) $M = 1.31$; (b) $M = 1.59$.

them further. These vortices however seem to travel around the vortex because they are located from 90° to 270° in Fig. 4(e). A circular weak shock forms around the vortex starting on the lower surface of the test model and ending perpendicular to the left part of the split reflected diffracted shock. It is not clear how it has generated but it is believed to be caused by the pressure gradients which occur after the vortex/shock interaction.

The main vortex, while growing in size, moves downstream from the wedge and holds a circular shape, when it starts to be flatten out in the vertical direction in Fig. 4(e). Transition to turbulence is evident since the vortex starts to lose its configuration, and in Fig. 4(f) the Kelvin–Helmholtz instability has been completely dampened out. As Fig. 5(d)–(f) illustrates, the shape of the vortex tends to become bigger and stretched in the horizontal direction as the Mach number increases and a counterclockwise rotation of its elliptical shape can be noted due to the higher incident flow velocity, which tends to incline the shear layer respect to the horizontal.

The vortex/shock interaction for Mach number of 1.59 develops faster (already visible in Fig. 5(c)), the expansion shock wave travels upstream slower, and the vortex increases in size changing shape more rapidly and transiting to turbulence earlier. This kind of interaction, depicted in Fig. 6(b), strongly affects the vortex evolution and has been named as strong vortex–strong shock interaction by Chang and Chang [25] causing the distortion of the vortex due to the transmitted wave which passes through it. Also the lambda waves on the slipstream disappear in Fig. 5(d) leaving only the last shocklet, which has increased its size with its tail joining an acoustic wave. Furthermore it can be observed that the contact surface does not roll up into the main vortex but seems to start from the second small vortex on the shear layer and it is slightly affected by the presence of the first one. This is also the point where a branch of the last lambda shock starts.

Similar to the case of Mach number of 1.31, the right-hand shock interacts with the shear layer in correspondence with a vortexlet forming a Mach reflection in Fig. 5(d)

and, later in Fig. 5(e), develops acoustic waves at a certain distance from the slipstream. A stronger stem starts in correspondence with the small vortexlet and tends to reach the vortex core. This flow structure is actually the part of the right-hand shock which is transmitted through the vortex and, since the flow speed on the inner part of the shear layer is lower than outside, it tends to travel slightly faster. Also the vortex/shock interaction on the left-hand side generates a structure with two shocks impinging the shear layer in correspondence with two small vortices which, in Fig. 5(e), merge into a unique shock that reaches the vortex core nearly symmetrically to the wave on the right-hand side.

3.2. Symmetrical geometry

The evolution of the shock wave diffraction around a symmetrical corner presents flow structures similar to the ramp case. Both the geometries can be grouped in the sharp shape category with the only difference that in the case of the symmetric corner the flow passes across a slight increase in area before being diffracted at the corner tip with the effect to accelerate it. However, as Fig. 7(a)–(c) shows, for a Mach number of 1.31 the absence of lambda shocklets indicates that the flow is still subsonic on the slipstream.

In comparison with the previous geometry, the development of the Kelvin–Helmholtz instability starts from Fig. 7(d), but now it tends to be more damped and completely disappears when a large number of small waves on the shear layer appear in Fig. 7(e) and (f). This wavelet structure develops after the diffracted shock, reflected from the test section wall, interacts with the vortex in the same manner as the previous case and indicates that the shear layer is less stable and develops some structures in the third dimension. A similar structure is illustrated in Fig. 8, which was obtained by Skews et al. [6] observing the evolution of the shear layer with a 30° convex corner noting a complex appearance of the shocklets. The arrangement and the amount of lambda shocks led the authors to think that they overlap along the spanwise direction.

In the case of a higher Mach number no relevant additional flow features were identified. The parallelism between

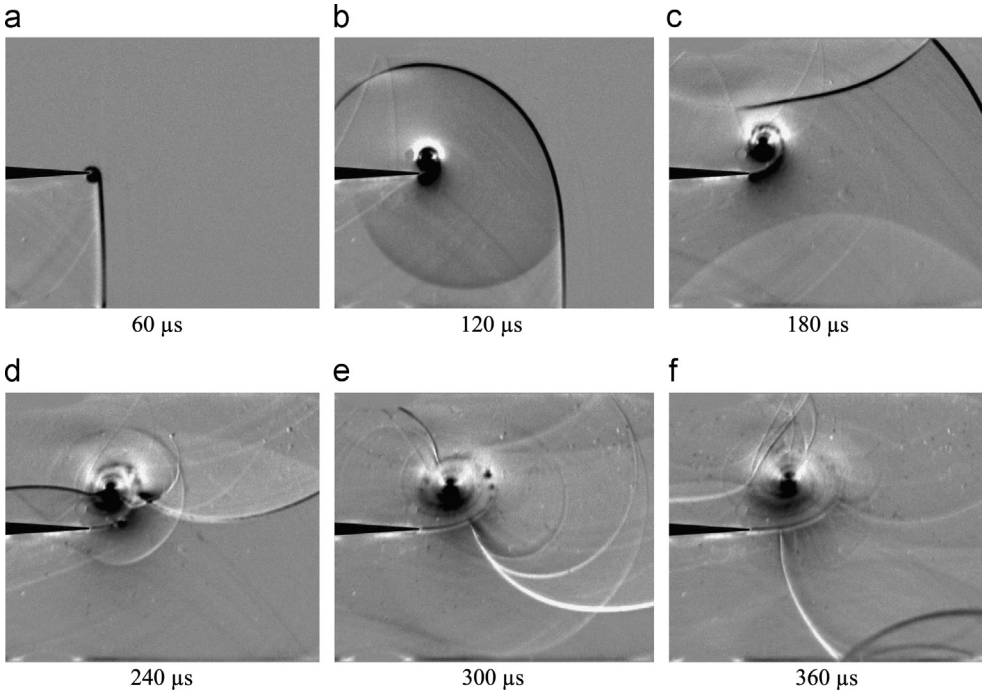

Fig. 7. Schlieren sequence of diffraction with an incident Mach number of 1.31 around a symmetric corner.

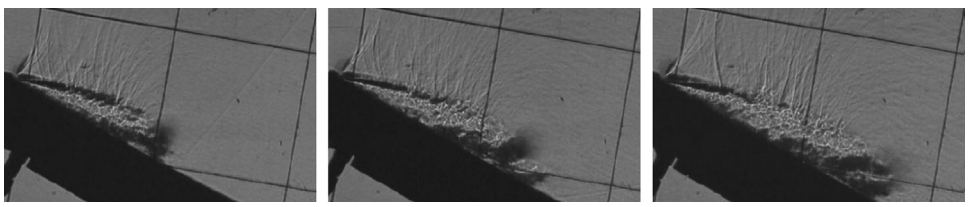

Fig. 8. Flow around a 30° corner at $M = 1.51$ at the delay time of 485, 685, 785 μs [6].

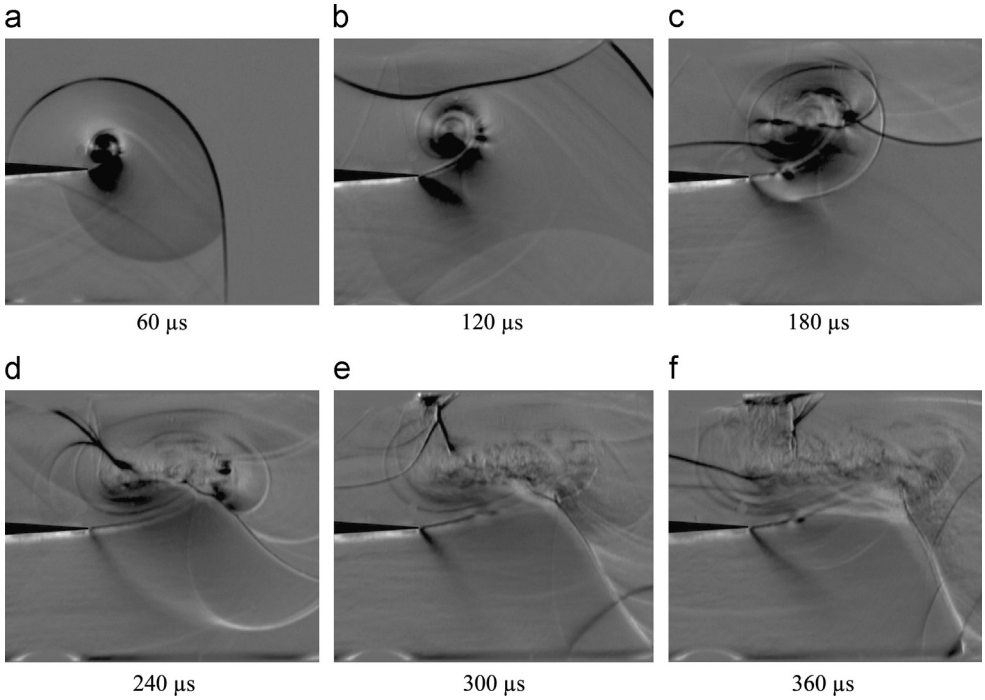

Fig. 9. Schlieren sequence of diffraction with an incident Mach number of 1.59 around a symmetric corner.

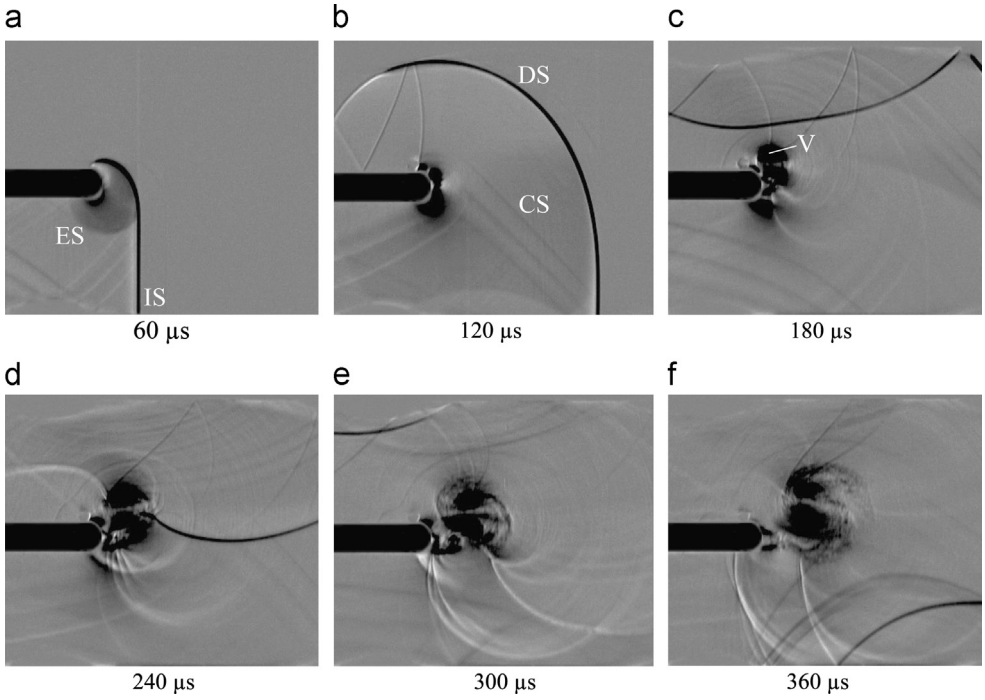

Fig. 10. Schlieren sequence of diffraction with an incident Mach number of 1.31 around a rounded corner.

Figs. 4 and 7, and Figs. 5 and 9 does not add any new insight to what has already been described for the previous geometry. The speed at which the diffraction process develops seems to be approximately in a good concordance with the ramp case since the flow structures appear to be identical and in the same position at the same time. The shear layer appears to be

rotated in the counterclockwise direction with respect to the centreline of the test window, but it is exactly the same if the lower surface of the model is positioned parallel to the test section walls.

3.3. Rounded geometry

The evolution of the shock wave diffraction process around a curved corner presents some differences compared to the sharp geometry. Fig. 10(a) and (b) illustrates the typical elements, i.e. the expansion sound wave which propagates upstream, the diffracted shock which appears to weaken while approaching the upper wall of the geometry model in Fig. 10(a), and the contact surface, that is clearly defined near the incident shock but not discernible in proximity of the wall as shown in Fig. 10(b).

The main difference compared to the sharp corners is the point where the shear layer separates, and for the Mach number of 1.31 a schematic of the flow is illustrated in Fig. 11(a). The incoming flow is accelerated on the curvature until it is not able to navigate any more and detaches from the surface, rolling up in the counterclockwise direction and forming the vortex. The detachment point occurs at a position Δ from the horizontal and therefore, differently from a sharp wedge, the Prandtl–Meyer expansion fan is not centred [8]. The small dimensions of the geometry and the limited resolution of the schlieren system allowed only a rough estimation of the distance Δ, which is greater for a higher Mach number.

The rounded geometry has also the effect that while the vortex grows in size, it remains close to the surface, where a convergent–divergent area is created, bounded by the corner and the shear layer, which acts as a wall. For Mach number 1.31 this is illustrated in Fig. 10(c). The flow around the main vortex is induced to pass through this channel where it is accelerated creating another point of detachment of the flow, similar to the previous one and named as internal shear layer by Quinn [7]. It was reported that this region locally reaches the supersonic range due to the area restriction between the wall curvature and the vortex and the necessity of the presence of an internal shocklet to slow down the flow rolling up into the vortex. The limitation of schlieren in the presence of steep gradients in density has not allowed us to properly observe the flow structure in this region and to not confirm the existence of this shock. Further studies with the combination of complementary diagnostic techniques are recommended [26,27]. In addition, according to Quinn [7], lambda shocks develop in the early stages of the process but not observed here, where instead some weak waves appear in Fig. 10(d) which start to travel upstream merging into a unique shock in Fig. 10(f). The number of these waves indicates an instability in the flow.

Comparing the flow evolution in the case of a lower Mach number, in Fig. 12(a)–(c), the shear layer and the vortex develop more rapidly. In this case the contact surface is visible in Fig. 12(a) and appears to be distorted by the presence of the vortex while approaching the wall in Fig. 12(b). This is in agreement with Skews [8], who noted that with rounded corners the contact surface never rolls up into the vortex independent of the Mach number. Fig. 12(b) also shows the convergent–divergent area illustrated in Fig. 10(c).

In analogy to the case of Mach number of 1.31, and as Fig. 11(b) schematically illustrates, the flow on the shear layer travels all around the vortex, passing then through the corridor between the test model and the slipstream, where is locally accelerated. This time the internal terminator, *InT*, can be clearly identified in Fig. 12(b) and the flow encounters two additional shock waves [7], namely secondary internal shock, *SInS*, which is linked with a lambda wavelet outside the slipstream, and recompression shock, *RS*, at 90° around the vortex which extends outside the corridor between the shear layer and the vortex, influencing the flow navigating on the slipstream. The presence of these three waves indicates that the induced flow reaches the supersonic speed and the necessity to slow it down to match the condition in the vortex core but, as the vortex starts to go away from the corner, the corridor enlarges and these waves begin to weaken completely disappearing from Fig. 12(d).

Some instabilities appear on the shear layer in Fig. 12(c) but seem to stop after the lambda shock, which does not generate in correspondence with the corner tip but a bit further from it. The complicated structure is due to the fact that the initial portion of the shear layer is perturbed by the presence of the internal slipstream creating a compression corner on the external shear layer where one

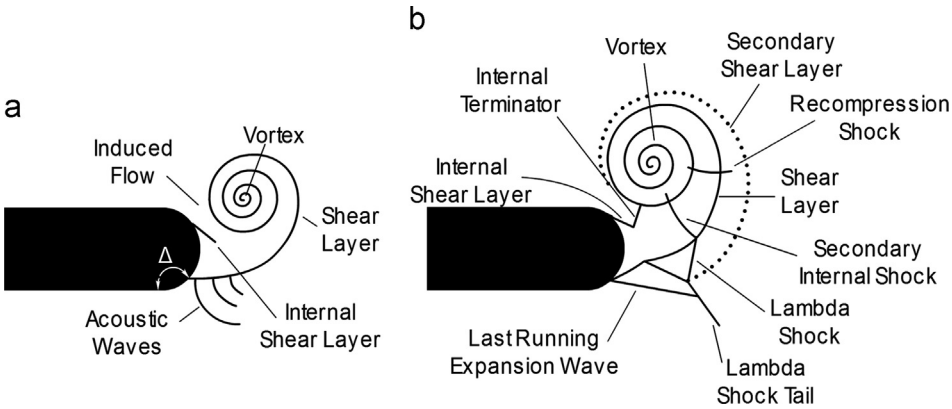

Fig. 11. Schematic of the shock wave diffraction around a curved corner for (a) $M = 1.31$; (b) $M = 1.59$.

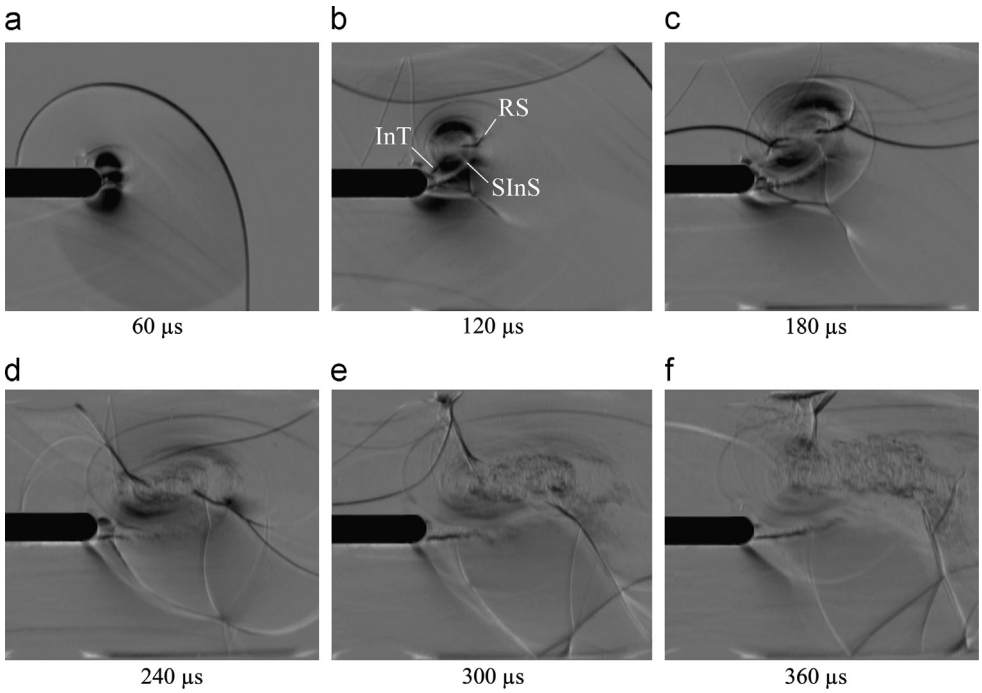

Fig. 12. Schlieren sequence of diffraction with an incident Mach number of 1.59 around a rounded corner.

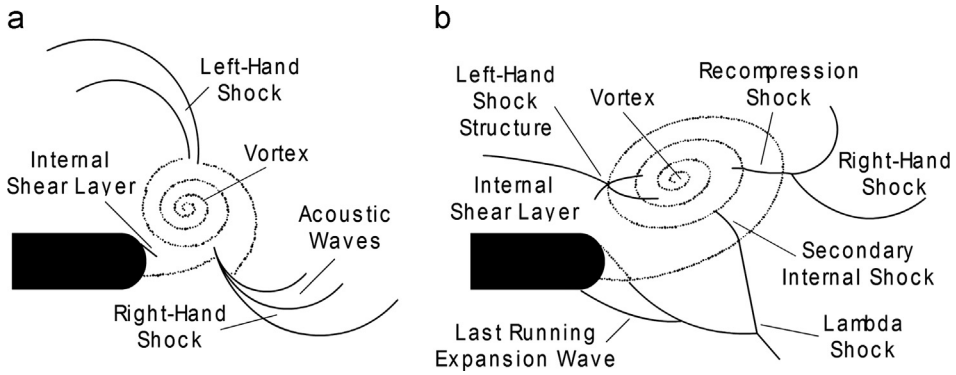

Fig. 13. Schematic of the vortex/shock interaction for a rounded corner at (a) $M = 1.31$; (b) $M = 1.59$.

branch of the lambda shock starts. Moreover on the wall, in proximity of the generating point of the slipstream, the incoming flow expands and the last running expansion wave joins the lambda shock on its tail.

For a Mach number of 1.31 the diffracted shock, after being reflected from the upper wall of the test section, returns to the splitter where it appears distorted in Fig. 10(c). The interaction, illustrated in Fig. 13(a), is not strong enough to cause the vortex displacement, whose shape appears still circular. The left-hand part is accelerated by the vortex rotation whereas the right-hand wave interacts with the shear layer penetrating it and developing a Mach reflection in Fig. 10(e), where also acoustic waves propagate. It is interesting to note that the point where the Mach reflection is generated seems to create a discontinuity on the shear layer: the shock on the right-hand side acts as a separator between the slipstream and the vortex and, from that point on, the vortex starts to travel downstream.

For a higher Mach number the vortex/shock interaction shown in Fig. 13(b) occurs in a strong fashion with the distortion of the vortex and the transmission of the wave through it. The shock eventually splits into two waves clearly visible in Fig. 12(c) and the one on the right-hand side merges with the recompression shock forming a Mach reflection on the slipstream and generates slightly perceivable diverging acoustic waves in Fig. 12(d) and (e). No vortices develop on the slipstream even though, differently from the sharp corners, it appears irregular and less smooth.

Lastly, a flow feature appears in Fig. 12(c), which was reported by Quinn [7] as secondary slipstream. This line, starting form the triple point of the lambda shock, travels all around the main shear layer and rolls up into the vortex. It acts as a boundary which separates the flow passing through the two branches of the lambda shock than that passing through the normal shock.

4. Conclusions

Schlieren has been used to qualitatively evaluate the development of a shock wave diffraction around three geometries with the result that the ramp and the symmetrical profiles behave in a similar manner and can be categorised as sharp wedges.

For rounded splitters the change in shape does not seem to contribute to a variation of the global speed of the phenomena evolution since the flow structures can be analysed in parallel with the sharp wedges in the range of Mach numbers tested. One peculiarity of this geometry is the formation of a convergent-divergent nozzle between the wall and the vortex. The acceleration of the flow in the corridor leads to the development of an internal shear layer and additional shock waves. Moreover, different from the sharp corners, the incoming flow is smoothly expanded on the surface before it separates at a certain distance, and the contact surface does not roll up into the vortex but ends on the splitter wall.

Schlieren photographs tend to obscure high-density regions, in particular the vortex core which, in the first images, is represented by a dark spot in all the cases tested. New mathematical methods currently under investigation are increasingly used to improve the accuracy and reliability of experimental data, such as the tomographic reconstruction of the density flow field around a body [28]. On the shear layer, only for a Mach number of 1.59, lambda structures appear, with a number and size dependent on the splitter geometry. Sharp corners are characterised by a well-defined vortex and a thin slipstream which easily develops the Kelvin–Helmholtz instability, whereas the greater thickness of the shear layer in the curved profile has a dampening effect.

The type of interaction was found to be strongly dependent on the vortex characteristics and the strength of the incoming flow. While for an incident Mach number of 1.59 the shock is always transmitted inside the vortex, at low speed the interaction is not strong enough to dislocate it and different geometries exhibit a dissimilar behaviour. In the sharp wedge the vortex remains compact whereas it appears more turbulent with a curved model tip.

Only one wedge angle in the sharp geometry and one radius in the curved corner were analysed. The similarity between the ramp and the symmetric splitters is a topic for further investigation to confirm if this trend is valid for any corner angle or only in a limited range of values. A test section with an increased vertical size is recommended in order to decrease the influence of reflected wave from the walls on the whole flow structure.

Acknowledgements

The authors are indebted to the EPSRC Engineering Instrument Pool, especially Mr. Adrian Walker for the loan of the high-speed camera. This work was supported by the Engineering and Physical Sciences Research Council [grant number EP/K504488/1.

References

[1] B.W. Skews, The perturbed region behind a diffracting shock wave, J. Fluid Mech. 29 (1967) 705–719.
[2] M. Sun, K. Takayama, A note on numerical simulation of vortical structures in shock diffraction, Shock Waves 13 (2003) 25–32.
[3] M. Sun, K. Takayama, The formation of a secondary sock wave behind a shock wave diffracting at a convex corner, Shock Waves 7 (1997) 287–295.
[4] H. Li, G. Ben-Dor, Z.Y. Han, Analytical prediction of the reflected-diffracted shock wave shape in the interaction of a regular reflection with an expansive corner, Fluid Dyn. Res. 14 (1994) 229–239.
[5] M. Sun, K. Takayama, Vorticity production in shock diffraction, J. Fluid Mech. 478 (2003) 237–256.
[6] B.W. Skews, C. Law, A. Muritala, S. Bode, Shear layer behavior resulting from shock wave diffraction, Exp. Fluids 52 (2012) 417–424.
[7] M.K. Quinn, Shock diffraction phenomena and their measurement (Ph.D. thesis), University of Manchester, 2013.
[8] B.W. Skews, Shock wave diffraction on multi-facetted and curved walls, Shock Waves 14 (2005) 137–146.
[9] G. Abate, W. Shyy, Dynamic structure of confined shocks undergoing sudden expansion, Prog. Aerosp. Science 38 (2002) 23–42.
[10] M.K. Quinn, K. Kontis, A combined study on shock diffraction, in: 5th Symposium on Integrating CFD and Experiments in Aerodynamics, Japan, 2012.
[11] B.W. Skews, The shape of a diffracting shock wave, J. Fluid Mech. 29 (1967) 297–304.
[12] G.B. Whitham, New approach to problems of shock dynamics, Part II: three-dimensional problems, J. Fluid Mech. 5 (1959) 369–386.
[13] D.S. Jones, G.B. Whitham, An approximate treatment of high-frequency scattering, in: Proceedings of the Cambridge Philosophical Society, vol. 53, 1957, pp. 691–701.
[14] T.V. Bazhenova, L.G. Gvozdeva, Yu.V. Zhilin, Change in the shape of the diffracting shock wave at a convex corner, Acta Astronaut. 6 (1977) 401–412.
[15] T.V. Bazhenova, L.G. Gvozdeva, M.A. Nettleton, Unsteady interactions of shock waves, Prog. Aerosp. Sci. 21 (1984) 249–331.
[16] M.J. Lighthill, The diffraction of blast. I, Proc. R. Soc. Lond. Ser. A: Math. Phys. Sci. 198 (1949) 454–470.
[17] R.S. Srivastava, On the vorticity distribution over a normal diffracted shock for small and large bends, Shock Waves 23 (5) (2013) 525–528.
[18] J.O. Reeves, B.W. Skews, Unsteady three-dimensional compressible vortex flows generated during shock wave diffraction, Shock Waves 22 (2012) 161–172.
[19] N. Gongora Orozco, H. Zare-Behtash, K. Kontis, Experimental studies on shock wave propagating through junction with grooves, in: 47th AIAA Aerospace Sciences Meeting Including The New Horizons Forum and Aerospace Exposition, 2009.
[20] N. Gongora Orozco, H. Zare-Behtash, K. Kontis, Particle image velocimetry studies on shock wave diffraction with freestream flow, in: 48th AIAA Aerospace Sciences Meeting Including The New Horizons Forum and Aerospace Exposition, 2010.
[21] H. Zare-Behtash, K. Kontis, N. Gongora Orozco, K. Takayama, Shock wave-induced vortex loops emanating from nozzles with singular corners, Exp. Fluids 49 (2010) 1005–1019.
[22] H. Zare-Behtash, N. Gongora Orozco, K. Kontis, Effect of primary jet geometry on ejector performance: a cold-flow investigation, Int. J. Heat Fluid Flow 32 (2011) 596–607.
[23] A.G. Gaydon, I.R. Hurle, The Shock Tube in High-temperature Chemical Physics, Chapman & Hall, London, 1963.
[24] J.D. Anderson, Modern Compressible Flow, with Historical Perspective, McGraw-Hill, New York, 1990.
[25] K.S. Chang, S.M. Chang, Scattering of shock into acoustic waves in shock-vortex interaction, Mater. Sci. Forum 465 (2004) 131–138.
[26] H. Zare-Behtash, N. Gongora-Orozco, K. Kontis, S.J. Holder, Application of novel pressure-sensitive paint formulations for the surface flow mapping of high-speed jets, Exp. Therm. Fluid Sci. 33 (5) (2009) 852–864.
[27] S.Z. Sapozhnikov, V.Y. Mityakov, A.V. Mityakov, R.L. Petrov, V.V. Grigor'ev, S.V. Bobashev, N.P. Mende, V.A. Sakharov, Heat flux measurements on the inner walls of a shock tube, Techn. Phys. Lett. 30 (1) (2004) 76–77.
[28] N.P. Mende, A.B. Podlaskin, V.A. Sakharov, An automated system for the image processing and reconstruction of the density field of an aerodynamic object, Tech. Phys. 45 (2) (2000) 251–254.